Pflugers Arch - Eur J Physiol (2014) 466:91–105
DOI 10.1007/s00424-013-1370-5

INVITED REVIEW

Physiology and pathophysiology of SLC12A1/2 transporters

Nicolas Markadieu · Eric Delpire

Received: 15 August 2013 / Revised: 21 September 2013 / Accepted: 23 September 2013 / Published online: 6 October 2013

Abstract The electroneutral Na^+–K^+–Cl^- cotransporters NKCC1 (encoded by the SLC12A2 gene) and NKCC2 (SLC12A1 gene) belong to the Na^+-dependent subgroup of solute carrier 12 (SLC12) family of transporters. They mediate the electroneutral movement of Na^+ and K^+, tightly coupled to the movement of Cl^- across cell membranes. As they use the energy of the ion gradients generated by the Na^+/K^+-ATPase to transport Na^+, K^+, and Cl^- from the outside to the inside of a cell, they are considered secondary active transport mechanisms. NKCC-mediated transport occurs in a $1Na^+$, $1K^+$, and $2Cl^-$ ratio, although NKCC1 has been shown to sometimes mediate partial reactions. Both transporters are blocked by bumetanide and furosemide, drugs which are commonly used in clinical medicine. NKCC2 is the molecular target of loop diuretics as it is expressed on the apical membrane of thick ascending limb of Henle epithelial cells, where it mediates NaCl reabsorption. NKCC1, in contrast, is found on the basolateral membrane of Cl^- secretory epithelial cells, as well as in a variety of non-epithelial cells, where it mediates cell volume regulation and participates in Cl^- homeostasis. Following their molecular identification two decades ago, much has been learned about their biophysical properties, their mode of operation, their regulation by kinases and phosphatases, and their physiological relevance. However, despite this tremendous amount of new information, there are still so many gaps in our knowledge. This review summarizes information that constitutes consensus in the field, but it also discusses current points of controversy and highlights many unanswered questions.

This article is published as part of the Special Issue on *Sodium-dependent transporters in health and disease*.

N. Markadieu · E. Delpire (✉)
Department of Anesthesiology, Vanderbilt University School of Medicine, MCN T-4202, 1161 21st Avenue South, Nashville, TN 37232, USA
e-mail: eric.delpire@vanderbilt.edu

Keywords SLC12A1/2 · NKCC1 · NKCC2 · Bartter's syndrome · Sensorineural deafness

Introduction

Evidence for an electrically neutral cotransport of Na^+, K^+, and Cl^- was first described in 1980 in Ehrlich ascites tumor cells [50]. This coupled transport of $1Na^+$, $1K^+$, and $2Cl^-$ was shown to be inhibited by furosemide, a diuretic used clinically to inhibit renal NaCl absorption in a specific part of the kidney tubule: the thick ascending limb of Henle (TAL) [56]. The molecular identification of two Na^+–K^+–$2Cl^-$ cotransporters, NKCC1 and NKCC2, was made in 1994 [28, 47, 62, 132], and the genes and exon structures were soon thereafter partially characterized [63, 105]. Expression patterns were examined by Northern blot analyses, in situ hybridization, and immunofluorescence studies once specific antibodies were generated against the cotransporters [61, 69, 70, 102, 135]. Effort was also made in generating NKCC1 [27, 37, 94] and NKCC2 knockout mice [117] to assess the consequence of eliminating protein expression on the physiology of these mice. While NKCC1 is ubiquitously expressed in cells and plays a major role in cell volume regulation and Cl^- secretion, NKCC2 is mainly expressed in the TAL where it mediates NaCl reabsorption. This review will examine the structure/function relationship, the physiological functions, and the regulation of the two Na–K–2Cl cotransporters.

Structure/function of SLC12A1/2 cotransporters

In humans, NKCC1 is encoded by the SLC12A2 gene which is present on chromosome 5q23, whereas NKCC2 is encoded by the SLC12A1 gene located on chromosome 15q15-q21. NKCC1 and NKCC2 form dimers, although each monomer

has been demonstrated to be fully functional [87, 115]. NKCC1 and NKCC2 monomers share overall 60 % sequence homology at the protein level (Table 1). NKCC2 is slightly smaller than NKCC1 with 1,099 amino acids yielding a core molecular size of 121.3 kDa, compared to 1,212 amino acids giving a size of 131.4 kDa [28, 47]. The main size difference results from a larger cytoplasmic N-terminal tail, which is some 102 amino acids longer in NKCC1. Consequently, the N-terminal tails are the least conserved portions of the two cotransporters (22 % amino acid identity). The regulatory cytoplasmic C-terminal tail and the core are well conserved between both isoforms with 56 and 79 % amino acid identity, respectively (see Table 1).

The cytosolic N-terminal tail

The N-terminal tail of NKCC1–2 is critical to cotransporter function. Deletion of the tail results in inactive cotransporters. However, as mentioned above, the amino terminal tail of NKCC shows the highest sequence diversity. This diversity is not only between NKCC1 and NKCC2, but also among the many NKCC1 orthologs whose sequences are found in GenBank (Fig. 1a and [45]). How can a domain with such diversity be so integral to transport function? The answer comes from two particular subdomains that are highly conserved within the Na^+-dependent cotransporters (NKCC and NCC). The first subdomain is a binding site for kinases, and the second subdomain consists of phosphorylation sites located near the plasma membrane. Sequences upstream of the kinase binding site and between the kinase binding site and the phosphorylation sites seem to be of less importance. We will discuss in a later section the regulation of NKCC1–2 by Ste20 (Sterile20) kinases and other regulatory proteins. In this section, however, we will briefly discuss the properties of these two highly conserved subdomains of the N termini. Using a yeast-two-hybrid analysis screen, we found that the N-terminus of cation–chloride cotransporters interacts with two specific Ste20 kinases: SPAK and OSR1. The site of interaction was reduced to nine amino acid residues containing a core RFXV (or RFXV/I) motif [101]. In fact, the tail of NKCC1 contains two such motifs, whereas the tail of NKCC2 only contains the first one. It is of interest to note that the second motif in NKCC1 overlaps with a PP1 binding motif, raising the possibility that the two proteins compete at that particular binding site [45]. Deletion mutants and site-directed mutagenesis studies demonstrated that only one motif was necessary for cotransporter activation, while the loss of the two motifs resulted in the absence of cotransporter function [45]. The presence of a PP1 binding motif in NKCC1 but not NKCC2 is puzzling. Studies have shown that NKCC1 activity is modulated by PP1 and mutation of this residue affects dephosphorylation of the cotransporter [22]. Results from our laboratory have also shown that binding of PP1 to the N-terminal tail of NKCC1 not only results in dephosphorylation of the cotransporter, but also to the dephosphorylation and inactivation of the Ste20 kinases [41, 46]. Once NKCC2 is activated by phosphorylation, it also needs to be dephosphorylated for inhibition. At this stage, it is not clear which phosphatase is involved and how it interacts with the N-terminal tail of NKCC2 and its phospho-sites. The second highly conserved subdomain is a peptide of 25–30 amino acids that contain multiple threonines and/or serine residues, some of which are targets of the kinases that bind to the upstream RFXV sites. Figure 1b highlights the information obtained from mass spectrometry/Edman sequencing analysis as well as site-directed mutagenesis studies. While several residues are involved, the most consistent residues are a pair of threonine residues separated by four amino acids: R/QT^{206}FGY/HNT^{211}M/I (numbers taken from mouse NKCC1). There are some interesting functional differences between the cotransporters at these two sites that are not yet explained. Indeed, mutation of T^{206} in NKCC1 completely abrogates cotransporter function [45], while mutation of the corresponding residue in NKCC2 reduced function by one third [55], and mutation in the Na–Cl cotransporter (NCC) has no functional effect [95]. Similarly, while mutation of T^{211} in NKCC1 [23, 45] and the corresponding residue in NCC [95] abolish cotransporter function, mutation of the corresponding residue in NKCC2 fails to do so [55]. Finally, note that no amino acid substitution of single or multiple threonine residues into either aspartic acid or glutamic acid residues, to mimic phosphorylation, confers constitutive activity to NKCC1. Instead, the substitutions disrupt cotransporter function [23, 45].

Table 1 Comparison between human NKCC1 and NKCC2

	hNKCC1		hNKCC2
Size (number of aa)	1,212		1,099
Size (MW in kDa)	121.3		131.4
Overall aa identity		60 %	
N-terminus aa identity		22 %	
C-terminus aa identity		56 %	
TM core aa identity		79 %	

Size of protein is given in number of amino acids and in kilodalton. Amino acid identity between isoforms is provided by domain

The transmembrane core

The core of the NKCC proteins consists of 12 hydrophobic transmembrane (TM) α-helices and a large extracellular loop between TM7 and TM8. The cation–chloride cotransporters belong to a large superfamily of transporters: the amino acid–polyamine–organocation superfamily, whose basic structure consists of an inverted repeat of five transmembrane domains

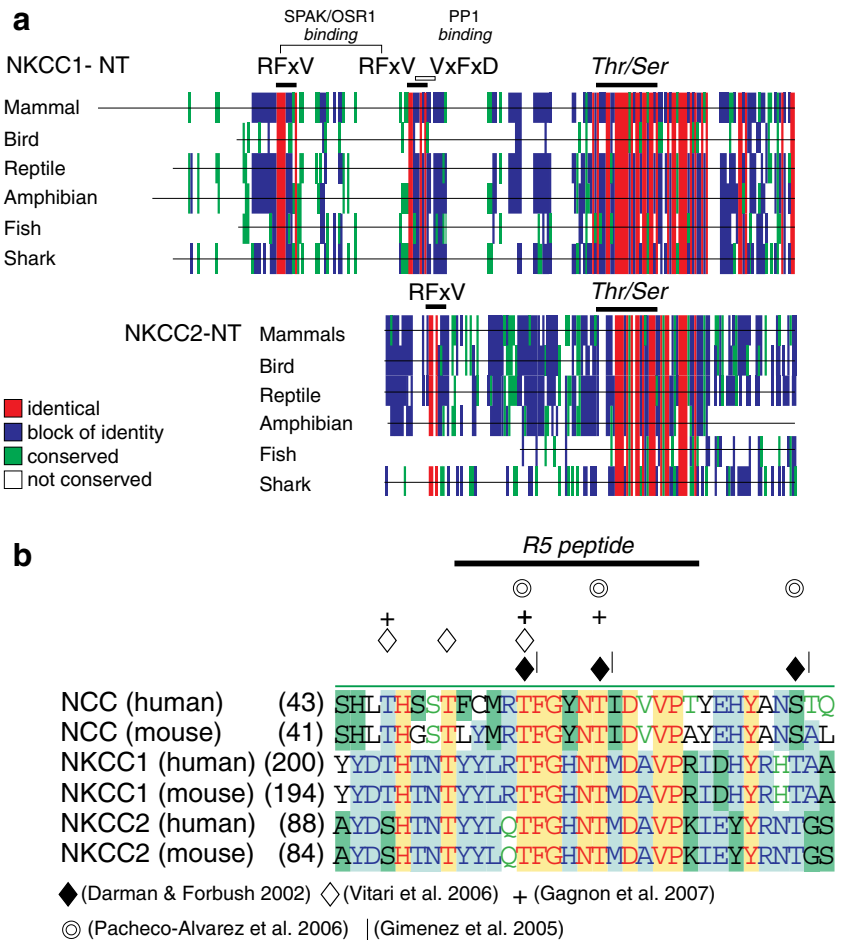

Fig. 1 Sequence homology and domains of the NH_2-terminal tails of NKCC1 and NKCC2. **a** Schematic comparison of NKCC1 and NKCC2 amino terminal tails from vertebrates: mammal (*Homo sapiens*), bird (*Gallus gallus*), reptile (*Anolis carolinensis*), amphibian (*Xenopus laevis*), bone fish (*Oreochromis niloticus*), and cartilage fish (*Squalus acanthias*). Identical residues are *highlighted in red*, conserved residues are *highlighted in green*, blocks of identical residues are shown in *blue*, and nonconserved residues are indicated in *white* (gaps). Note the presence of two to three regions of high degree of conservation, corresponding to the SPAK/OSR1 binding motifs, and the phospho-threonines and phospho-serines. *Bars* indicate the RF*x*V motifs or SPAK/OSR1 binding site (*filled bar*), and the V*x*F*x*D motif or PP1 binding site (*open bar*). **b** Amino acid alignment of a portion of the N-terminal tail of human and mouse NCC, NKCC1, and NKCC2. Protein sequences were aligned using VectorNti (Invitrogen) and a portion of the alignment is displayed. Threonine and serine residues that are targets of phosphorylation are highlighted with references. The position of the R5 peptide used to generate the R5 antibody [38] is indicated. Residues *highlighted in yellow* are identical residues, whereas amino acids *highlighted in green/blue* represent conserved residues

followed by two additional transmembrane α-helical segments at their N- and/or C-termini [129]. The Phyre^2 protein fold recognition server (www.sbg.bio.ic.ac.uk/phyre2/) drew a model (>90 % confidence) of the first 10 transmembrane domains of NKCC1, which is represented in Fig. 2a. The model is based on structure similarity with several resolved structures (Protein Data Bank IDs: 4dji, 3gia, 3lrc, 2jln, and 3dh4). A characteristic of amino acid–polyamine–organocation transporters is the duplication or repeat of five transmembrane domains. This 5+5 symmetry can be seen with pairs of TM1–TM6, TM2–TM7, TM3–TM8, and TM4–TM9 being in close proximity of each other, whereas TM5 and TM10 being separate (Fig. 2a, b). To further demonstrate the 5+5 symmetry, we aligned the five first TMs with the next five and significant amino acid conservation is observed (Fig. 2c). Note the conservation of two pairs of residues between TM2 and TM7, the SV and MM residues in TM2 having been shown to participate in cation binding (see below). While the hydropathy plots of NKCC reported in multiple studies [28, 47, 52, 132] diverges somewhat from that of LeuTAa, a bacterial homolog of neurotransmitter sodium symporters belonging to the same amino acid–polyamine–organocation superfamily, there are some striking high spots of conservation. For instance, four of the six residues in TM9 and 7 out of 10 residues in TM12 that have been shown to promote cotransporter dimerization [134] are conserved in NKCCs. Glycosylation of the large TM7–TM8 loop increases the molecular size of NKCC1 and NKCC2 by some 30–40 kDa [90] and is essential for membrane expression, transport activity, and affinity for loop diuretics [97]. Indeed, inhibition of glycosylation by tunicamycin drastically reduces

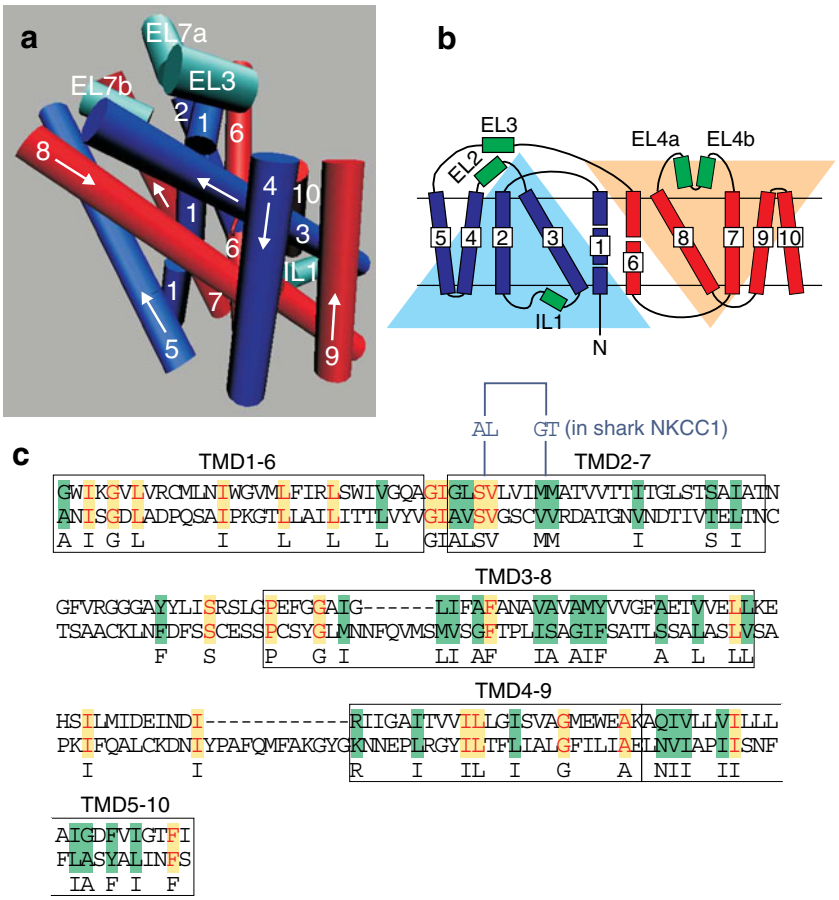

Fig. 2 Structure of the core of human NKCC1. **a** Structure of the transmembrane domains and other alpha helices was modeled using the Phyre[2] protein fold recognition server [72]. The PDB file was viewed using the Visual Molecular Dynamics software (University of Illinois) and the image was rendered after highlighting the α-helices. The first five TMs are colored in *blue*, whereas the next five TMs are colored in *red*. Note the proximity and parallelism of TM1–6, TM2–7, TM3–8, and TM4–9. **b** Predicted topology of the first 10 transmembrane domains based on similarity to crystal structure of amino acid–polyamine–organocation transporters. The last two transmembrane domains are not drawn. **c** Alignment of two segments of the human NKCC1 core showing conservation of transmembrane domains. The SV and MM/VV amino acids in human NKCC1 TMD2–7 are replaced by AL and GT in shark NKCC1. The alignment was done with VectorNti 6 (Invitrogen)

the activity of both cotransporters. Site-directed mutagenesis of the two N-linked glycosylated sites (N442Q, N452Q) of NKCC2 reduces its membrane expression and activity when single or double mutants are expressed in the heterologous *Xenopus laevis* oocyte system. While cation affinity was unchanged in mutants versus wild-type NKCC2, Cl^- affinity was increased and binding of the loop diuretic bumetanide was decreased in the single N442Q and double N442Q/N452Q mutants. Interestingly, the N442 glycosylated site is conserved in NKCC1, and its mutation also confers an increase in Cl^- and a decrease in bumetanide binding [97]. This observation suggests that a reduction in the net negative charge at the extracellular surface of both cotransporters, induced by the absence of glycosylation, increases Cl^- affinity but decreases inhibition by loop diuretics. Moreover, the fact that bumetanide and Cl^- affinity are significantly modified when glycosylation is prevented, could imply that the loop diuretic and the Cl^- binding sites are located near the N422 residue. Taking advantage of differences between the living environments of men and sharks, and consequently of a several fold difference in ion binding affinities between human NKCC1 and shark NKCC1, Biff Forbush's group created chimeras to map the ion binding domains on the cotransporters [66]. They demonstrated that the Na^+ affinity of NKCC1 was 15 mM in human versus 109 mM in shark. The sequence of shark NKCC1 TM2 differs from human NKCC1 TM2 at the two pairs of residues highlighted in Fig. 2c (AL residues instead of SV and GT residues instead of MM). Substitution of these pairs of residues in the shark sequence by their human counterparts significantly decreased the affinity for both Na^+ and K^+ ions [66]. It is worth noting that similar to TM2, TM7 is also involved in cation binding [65], which is consistent with the symmetry model (Fig. 2a or b). As NKCC1 is inhibited by bumetanide, the chimeric approach was also used to map residues affecting bumetanide binding. It was shown that multiple transmembrane domains (TM2, 11, and M12) participate in bumetanide binding [65]. Recently, cysteine- and tryptophan-scanning mutagenesis experiments have shown that TM3 also plays a major role in ion translocation and binding of loop diuretics [114]. Additional studies are required to specify the role of each transmembrane domain and identify amino acids involved in ion and loop diuretics binding in both cotransporters.

The chimeric approach was also used to decipher the molecular basis for the high osmolarity/volume sensitivity of NKCC1 versus low osmolarity/volume response of NKCC2. The Na–K–2Cl cotransporter has been known for many decades to be activated by hypertonicity or cell shrinkage (for an

early review, see [49]). We noticed, however, a significant difference in the level of activation from 3- to 4-fold increase in K^+ influx for NKCC1 versus 1.5-fold increase for NKCC2 [40]. While the activation requires phosphorylation of the N-terminal tail (see above), we demonstrated that swapping the tails of the cotransporters did not affect their level of activation. In contrast, we showed that portions of the protein that includes the second transmembrane domain (TM2) along with the first intracellular loop (IL1) and the second extracellular loop (EL2) "encode" for the high sensitivity of NKCC1. It is of significance that not only the transmembrane domain but also the loops are involved in the fold activation [40].

With the exception of the squid axon NKCC1, whose stoichiometry of transport was shown to be $2Na^+:1K^+:3Cl^-$ [109], the typical stoichiometry for both NKCC1 and NKCC2 is $1Na^+:1K^+:2Cl^-$ [50]. However, when we measured unidirectional K^+ and Cl^- influxes in NKCC1-injected oocytes exposed to hypertonicity, we observed identical ion fluxes [40]. This was interpreted as NKCC1 functioning partially in K^+/K^+ exchange mode. Two kinetics models have been described for NKCC1 [26, 81]. The first complete model of ion binding to NKCC1 came from studies performed in duck red cells [81, 85]. It was shown that the free transporter binds Na^+ first, followed by Cl^-, then K^+ and the second Cl^- (Fig. 3a). Interestingly, it was postulated that the order of ion release on the other side is reversed so the first ion attached to the cotransporter would come off first. This postulate gave rise to a gliding model, conceptually different than the symmetrical model [81]. Note that K^+/K^+ exchange in this model can be explained if, close to the end of the cycle, the partially unloaded transporter picks a K^+ ion and reverses its orientation (Fig. 3a, red arrows). This model has remained unchallenged until we observed kinetic behavior better compatible with a model where the transporter binds Cl^- first, followed by Na^+, the second Cl^- and then K^+ (Fig. 3b). In this model, K^+/K^+ exchange can still occur when partially loaded carriers reverse their orientation and re-load K^+ ions. Note that an unusual NKCC1 stoichiometry has also been measured in neonatal neurons [9].

Both NKCC1 and NKCC2 are capable of transporting alternative ions as substitute for K^+ and Cl^-. For instance, rubidium (Rb^+) is often used in its radioactive form (^{86}Rb) as a tracer for K^+ because the isotope half-life is far more convenient than isotopes of K^+, and the cotransporter affinity for Rb^+ is similar to that of K^+ (discussed in [26]). Thallium (Tl^+) has been recently used in combination with intracellular fluorescent dyes to assess the function of NKCC1 and NKCC2 [17, 25, 51]. To date, how Tl^+ affinity compared to that of K^+ is unknown. NH_4^+ can also substitute for K^+ and be inwardly transported by both cotransporters. Fast accumulation of NH_4^+ within the cell results in acidification of the intracellular pH, which in turn, inhibits the activity of the cotransporters [7]. Note that, as it will be described below, NKCC2 in the kidney and NKCC1 in the intestine regulate acid–base balance

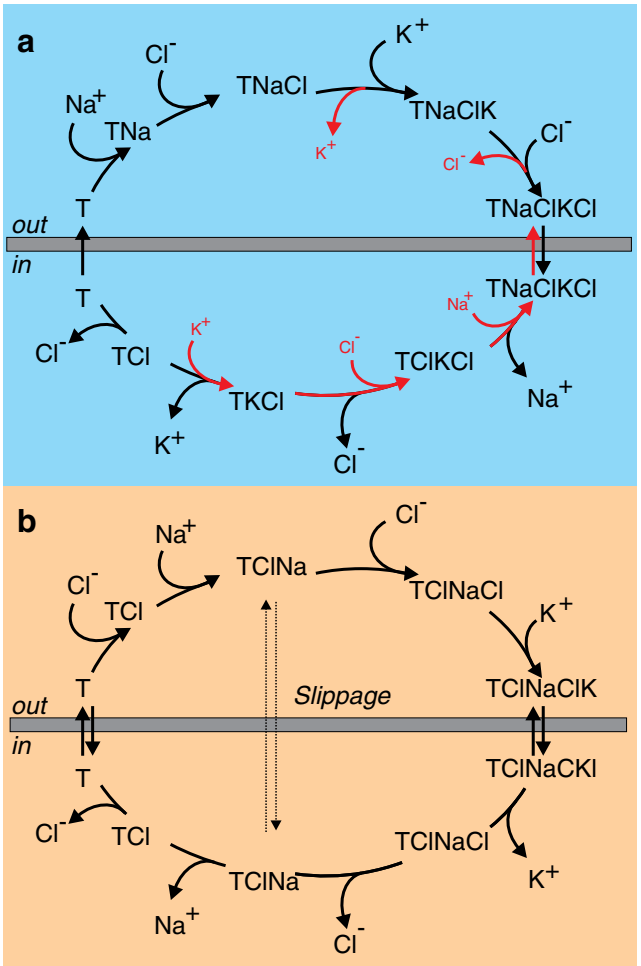

Fig. 3 Two kinetic models of Na–K–2Cl cotransport. **a** Glide symmetry model where a Na^+ ion binding first *on* the cotransporter in the outside facing configuration is the first ion coming *off* in the inward facing configuration. **b** Alternative model with more conventional kinetics where Cl^- binds first followed by Na^+, the second Cl^-, and K^+. Partial reactions or slippages which are electroneutral in nature (e.g., NaCl movement) are allowed. See text for details and references

by promoting NH_4^+ transport. As far as the anions are concerned, Br^- substitutes quite well for Cl^- on NKCC1, whereas I^- is a poor substitute for Cl^- (see Fig. 4). Note, however, that the cotransporter is able to mediate some K^+ movement in the presence of iodide, as we were able to measure a small but significant bumetanide-sensitive K^+ influx in the presence of this anion.

The cytosolic C-terminal tail

The C-terminal tails of NKCC1 and NKCC2 are important for maturation, dimerization, and protein trafficking to the plasma membrane. While no splicing events involving the C-terminal tail of NKCC2 have been reported, there is one isoform of NKCC1 that has a different carboxyl-terminus. The alternatively spliced isoform involves a cassette exon (exon 21 which

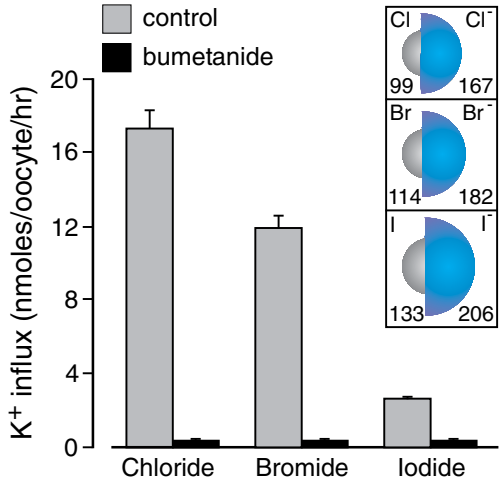

Fig. 4 NKCC1 transport of Cl^-, Br^-, and I^-. K^+ influx was measured in NKCC1-injected *Xenopus laevis* oocytes in a hyperosmotic solution containing 96 mM NaCl, 4 mM KNO_3, 2 mM $Ca(NO_3)_2$, 1 mM $MgSO_4$, 60 mM sucrose, and 1 mM ouabain in the presence or absence of 20 μM bumetanide (pH 7.4, osmolality 260 mOsM). For halide substitution, NaCl was replaced with NaBr, or NaI. Fluxes are expressed in nanomoles K^+ per oocyte per hour. *Bars* represent means±SEM (n=20–25 oocytes). *Values in inset* represent sizes (radius) of atoms and their ions in pm

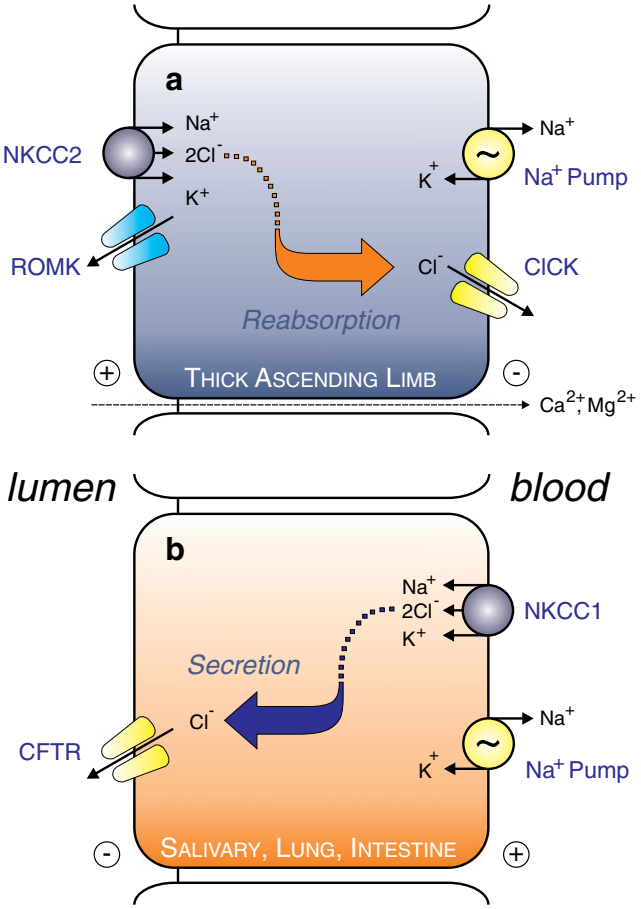

Fig. 5 Na–K–2Cl cotransport in two types of epithelial cells. **a** Thick ascending limb epithelial cell model showing apical NKCC2 localization. The driving force for NaCl reabsorption is provided by the basolateral Na^+/K^+ pump. Apical K^+ channel (ROMK) delivers K^+ in the lumen for NKCC2 function and creates an electropositive lumen. $ClCK_{(A\ and\ B)}$ on the basolateral membrane creates a path for Cl^- movement and participate in the electronegative blood side. The electrical field generated by the epithelial cells favors the paracellular reabsorption of divalent cations. **b** Model of a Cl^- secreting epithelial cell with localization of NKCC1 on the basolateral membrane. The cotransporter replenishes Cl^- as the anion is transported across the apical through CFTR or other Cl^- channels. K^+, which enters through the pump and NKCC1, leaves the cell through apical and basolateral K^+ channels (not shown). Note that this model can be used for stria vascularis marginal cells (K^+ secreting cell) with CFTR substituted for KCNQ1

is 48-bp-long and encodes 16 amino acids) which is omitted in some tissues [105, 122]. Although the 3′ end of the exon creates a PKA consensus site when present, there is no evidence that protein kinase A modulates NKCC1 function at that locus. In contrast, the 16 amino acids fragment was shown to contain a di-leucine motif as a basolateral sorting motif, therefore targeting NKCC1 to the basolateral membrane of epithelia [13]. This sequence is absent in both the NKCC1 isoform lacking exon 21 and NKCC2. Absence of the basolateral targeting sequence explains the apical localization of NKCC2 in the thick ascending limb of Henle. When we identified the alternatively spliced isoform of NKCC1 in 1997, we found it to be abundant in the brain. Whether or not the apical localization of NKCC1 in choroid plexus [102, 131] is due to the absence of exon 21 is unknown. The C-terminal tail of NKCC1 has been shown to facilitate di- and tetramerization of the cotransporter. This was shown using a yeast-two-hybrid method [111] and fluorescence resonance energy transfer (FRET) analysis [86].

Physiological functions of the SLC12A1/2 cotransporters and relation to human diseases

NKCC2

NKCC2 is expressed on the apical membrane of the epithelial cells of the thick ascending limb of Henle (TAL) which reabsorbs about 20–30 % of the NaCl filtered by the glomerulus ([4], Fig. 5a, Table 2). Note that the main function of the TAL is to reabsorb large amount of NaCl while reabsorbing no water, which leads to dilution of the forming urine in the tubule lumen [6, 82]. Loss-of-function mutations in SLC12A1 gene result in Bartter's syndrome, an autosomal recessive disease characterized by plasma volume reduction, polyuria, hyponatremia, hypotension, hypochloremia, hypokalemia, magnesuria, metabolic alkalosis, and hypercalciuria [11, 112]. These multiple characteristics can be explained as follows: a decrease in Na^+ reabsorption in the TAL results in an increased delivery of Na^+ in the collecting duct, where its reabsorption is mediated by the epithelial Na^+ channel, ENaC. Increased ENaC activity results in an increased K^+ secretion by the channel ROMK [78], leading to hypokalemia and gives rise to an increased H^+ secretion by intercalated cells

Table 2 Functions of NKCC1 and NKCC2

NKCC1		NKCC2	
Localization	Function	Localization	Function
Inner ear	Hearing and balance	Kidney: TAL	Na^+ reabsorption, NH_4^+ reabsorption
Sensory neurons	Filtering sensory noise	Kidney: macula densa	Na^+ sensing (tubuloglomerular feedback)
CNS neurons	Proconvulsant or anticonvulsant		
Salivary gland epithelial cells	Salivary volume		
Intestine interstitial Cajal cells	Peristalsis		
Vascular smooth muscle cells	Vascular tone		
Testes	Spermatogenesis		
Airway epithelial cells	Maturation of fetal lung		
Distal colon	NH_4^+ secretion		

H^+-ATPase, leading to metabolic alkalosis [124]. Furthermore, the decrease in plasma volume associated with the defect in TAL Na^+ reabsorption stimulates the renin–angiotensin–aldosterone system leading to an increased production of angiotensin II and aldosterone which respectively stimulates proximal Na^+/H^+ exchanger and distal ENaC, thereby leading to a further secretion of H^+ and K^+ [74]. This phenotype has been mostly reproduced in a mouse model [117]. The homozygous NKCC2 knockout mice exhibit a severe decrease in plasma volume, high plasma renin, hypokalemia, and metabolic alkalosis, while heterozygous knockout mice did not show any physiological difference when compared with wild-type mice. Reversely, enhanced activity of NKCC2 has been linked to hypertension and hypertensive disorders in rodents and in humans [12, 15, 118].

NKCC2 is also present in the apical membrane of the macula densa, which is located in the juxtaglomerular apparatus and is strategically in contact with the distal tubule and the extraglomerular mesangium close to the afferent arteriole [70]. The macula densa cells are NaCl sensors able to adjust the glomerular filtration by vasodilatation or vasoconstriction of the afferent arteriole. While a decrease in tubular NaCl concentration results in vasodilation of the afferent arteriole and in renin release by the granular cells, an increase in NaCl concentration induces a vasoconstriction of the afferent arteriole and thereby a decrease in glomerular filtration. This latter mechanism is known as the tubuloglomerular feedback and NKCC2 has been shown to play a pivotal role in the sensing of this high tubular NaCl concentration ([100, 110], Table 2). Note that NKCC1 is also highly expressed in the afferent arteriole renin-positive cells and in juxtaglomerular mesangium [69], possibly also related to tubuloglomerular feedback.

Alternative splicing of the exon 4 of the SLC12A1 gene gives rise to three NKCC2 variants [61, 98]. These variants have different transport characteristics and different localizations along the TAL and the macula densa (Fig. 6). NKCC2F, which is the most abundant variant, is exclusively expressed in the medullary TAL, while NKCC2A is detected in both medullary and cortical TAL and NKCC2B is present in the cortical TAL. Macula densa express both NKCC2A and NKCC2B. Note that in human, NKCC2A is the predominant variant, possibly a reflection of a slightly different diet and physiology [18]. Affinity for Cl^- differs between variants, and although there is some variability between species, the sequence order is NKCC2B> NKCC2A>NKCC2F for mouse and rabbit cotransporters [19].

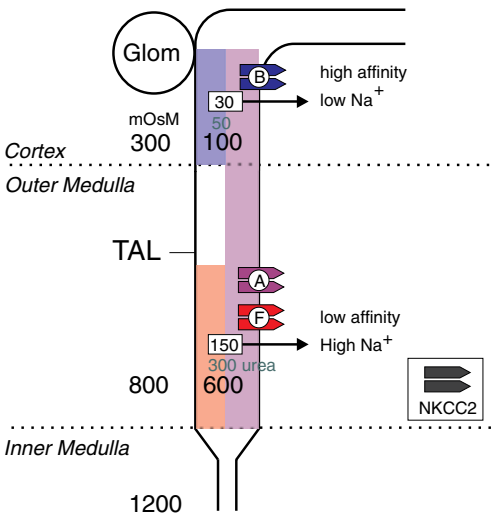

Fig. 6 Diagram of the mouse medullary and cortical thick ascending limb of Henle expressing NKCC2. The low affinity isoform, NKCC2F, is expressed in the lower portion of the outer medullary TAL where the urine Na^+ concentration is high. The high affinity isoform, NKCC2B, is expressed in cortical TAL where the urine Na^+ concentration is low. The intermediate affinity isoform, NKCC2A, is expressed along the entire TAL. In the outer medulla, the major role of NKCC2 is to transport Na^+ without water, thus raising the osmolarity of the interstitium. Osmolarity of the urine and interstitium and the urea and Na^+ concentrations in the urine are provided. *Glom* glomerulus

The presence of both NKCC2A and B variants in the macula densa facilitates efficient NaCl sensing over a wide range of fluctuating NaCl concentrations [18, 19]. Specific NKCC2 variant knockouts did not show severe salt-wasting phenotype probably because of compensation by the other NKCC2 variants [93].

NKCC2 is also a major player in NH_4^+ reabsorption and acid–base homeostasis (Table 2). NH_3 is produced by glutamine metabolism in renal epithelial cells and exists predominantly in its acidic form, NH_4^+, at physiological pH. The proximal tubule is primarily responsible for luminal NH_4^+ secretion, which is substantially increased by metabolic acidosis. Thereafter, NH_4^+ is reabsorbed in the TAL by NKCC2 and, subsequently, accumulated in renal interstitium where it contributes to the high medullary osmolarity. It is finally secreted back into the urine by Rhesus glycoproteins in the collecting duct [73, 126].

NKCC1

In contrast to NKCC2, which exhibits a highly restricted pattern of expression, NKCC1 is widely expressed in human, mouse, and other vertebrates. To date, there are no mutations that have been found in the human SCL12A2 gene, which suggests that loss of NKCC1 function might be embryonic lethal in human. Considering the many tissues and functions supported by NKCC1 (see Table 2), it is surprising that the NKCC1 knockout mouse is viable [27, 30, 37, 94]. The most striking deficit of the NKCC1 knockout mouse is sensorineural deafness and imbalance, which originates in cochlea and semicircular canals and vestibule, respectively. In the cochlea, the stria vascularis stratified epithelium composed of marginal cells expresses the Na^+/K^+-ATPase and NKCC1 on the basolateral membrane. As in many epithelia, the Na^+/K^+ pump provides the force for K^+ and Cl^- influx through NKCC1. While Na^+ and Cl^- are subsequently recycled respectively through the Na^+/K^+ pump and the ClCK Cl^- channel, K^+ is secreted into the scala media by the complex of K^+ channels: KCNQ1/KCNE1 [75, 89, 121]. The high potassium endolymph generates a positive (+85 to +100 mV) endocochlear potential with a large driving force for the movement of K^+ into sensory hair cells, which transduce mechanical into electrical signals [138].

NKCC1 is also highly expressed in inner ear spiral (cochlear) and vestibular ganglia [27]. While the role of the cotransporter in these specific neurons is unknown, this observation is interesting in light of the role that NKCC1 plays in sensory afferent neurons. In primary afferent neurons of dorsal root ganglia, NKCC1 participates in Cl^- accumulation in both the neuronal cell body and axon terminals. High Cl^- in the terminals leads to GABA depolarization, presynaptic inhibition, and filtering of sensory noise [2, 116, 128]. As $GABA_A$ receptor subunits are also very abundant in rat spiral ganglion [133], it is tempting to speculate that the cotransporter in inner ear ganglion neurons might be participating in the filtering of auditory noise.

Regulation of intracellular Cl^- seems to be an important function of NKCC1 in adult neurons located outside the central nervous system (CNS). NKCC1 is abundant not only in primary afferent dorsal root ganglion and inner ear neurons, but also in olfactory neurons [107] and gonadotropin releasing hormone neurons [24]. In contrast in the CNS, NKCC1 expression is only elevated in immature neurons but then decreases during neuronal maturation [32, 103]. The role of the cotransporter in immature neurons is, however, not very well understood. First, there is currently a debate in the field on whether the cotransporter truly accumulates Cl^- in immature neurons. In reality, only minimal changes in the GABA-mediated Cl^- reversal potential are measured in wild-type neurons exposed to bumetanide [32, 140] or in neurons lacking NKCC1 expression versus wild-type neurons [5, 139]. Second, there is conflicting information regarding the pro- versus anticonvulsant nature of the cotransporter as studies have demonstrated that bumetanide decreases spontaneous network activity in the immature hippocampus [32], whereas absence of NKCC1 significantly increased spontaneous activity in immature CA3 pyramidal neurons [140]. Bumetanide treatment has been recently effectively used in treating adult patients with temporal lobe epilepsy [33]. However, it is difficult to know if the effect of the loop diuretic is a direct effect on neurons or an indirect effect due to volume depletion. Indeed, the diuretic in the circulation is bound to albumin and does not permeate the blood–brain barrier. The diuretic is currently in clinical trial for intractable neonatal seizures (http://ClinicalTrials.gov). In these newborns, the blood–brain barrier might not be completely tight and the diuretic might be crossing to the brain.

NKCC1 also plays an important role in epithelial function (Fig. 5b). In salivary gland, NKCC1 is highly expressed at the basolateral membrane of acinar cells where it participates in the secretion of fluid that accompanies secreted α-amylase and mucine. Inhibition or deletion of NKCC1 gives rise to a reduction in the volume of saliva secreted in response to muscarinic agonists [34]. In the intestine, the cotransporter is expressed on the basolateral membrane of epithelial cells where it is also involved in fluid secretion [37, 67, 91]. Interestingly, the cotransporter is also expressed in cells involved in peristalsis or contraction and relaxation of smooth muscles that helps the movement of the food along the gastrointestinal tract. Indeed, the cotransporter is found in the interstitial cells of Cajal which surround the myenteric plexus and serve as a pacemaker. These cells generate slow waves that synchronize smooth muscle cell contraction, thus promoting an efficient intestinal transit. NKCC1 is responsible for maintaining intracellular Cl^- concentration above equilibrium and its absence in NKCC1 knockout mice induces a

depolarization of the smooth muscle cell membranes, leading to a decrease in the frequency and amplitude of the slow waves. In wild-type cells, bumetanide reversibly affects the shape, frequency, and amplitude of slow waves in the smooth muscle cells of the jejunum [130]. Deficit in peristalsis in the NKCC1 knockout mouse might explain the intestinal obstructions and high lethality observed in animals prior to weaning [37]. In humans, impaired myenteric cells of Cajal have been reported in chronic intestinal pseudo-obstruction, infantile pyloric stenosis, Hirschsprung's disease, slow transit constipation, and diabetic gastroparesis [35, 119, 120, 125].

Two additional striking phenotypes of the NKCC1 knockout mouse are hypotension and male infertility. The hypotension is due to decreased vascular tone, as studies performed in isolated rat aorta have shown that NKCC1 is activated by vasoconstrictors, inhibited by nitrovasodilators, and is upregulated in hypertension [37, 48]. Furthermore, intravenous infusion of bumetanide resulted in a rapid drop in blood pressure in wild-type mice, but not in NKCC1 knockout mice [48]. NKCC1 knockout males show smaller testis size than their wild-type counterpart. Histological analysis demonstrates a smaller diameter of the seminiferous tubules and absence of mature spermatids near the lumen of the tubule [94]. This deficiency might be due to a deficit in the hypothalamus/pituitary/testis axis, as reduced circulating levels of testosterone and luteinizing hormone are observed in the knockout mice [43].

Regulation of SLC12A1/2

Regulation of the gene level

In contrast to other transport mechanisms, there is very little information about the regulation of the SLC12A1/2 genes at the transcriptional level. The SLC12A2 gene (NKCC1) is encoded by 28 exons, and as discussed above, exon 21 is alternatively spliced. Analysis of the genomic DNA sequence upstream of the putative transcriptional initiator site revealed a promoter region characteristic of a housekeeping gene: a TATA-less promoter and several Specificity Protein 1 (Sp1) sites [105]. Activator protein-2 (AP-2) binding sites are also located ~30 and ~500 bp upstream of the transcription initiator site. In plants, AP-2 transcription factors have been implicated in response to environmental signals in stress acclimation [29]. AP-2 s are also involved in the regulation of cell proliferation, differentiation, apoptosis, and carcinogenesis [99]. Several studies have examined changes in NKCC1 mRNA/protein expression upon changes in physiological conditions. Experiments performed in rats dehydrated for 2 days or fed with NH_4Cl for 6–7 days to induce metabolic acidosis have shown a significant increase in NKCC1 abundance in both outer and inner medullary collecting ducts [64]. In another study performed in cell culture with T-84 cells, it was shown that hypoxia leads to a significant decrease in NKCC1 transcription [60]. This decrease was due to HIF-1α, a transcription factor mediating transcriptional activation of genes in response to decreased oxygen concentration [92]. Colonic mucosal scrapings from HIF-1α knockout animals showed a ~10-fold increase in NKCC1 expression [60]. Finally, NKCC1 expression was shown to be significantly downregulated in a skin-specific knockout of the forkhead transcription factor, FoxA1 [21]. NKCC1 expression is also epigenetically regulated during the development of hypertension in rat models [20]. While the NKCC1 promoter is methylated with age in normotensive rats, the promoter is hypomethylated in spontaneous hypertensive (SHR) rats. Hypomethylation of the NKCC1 promoter leads to an increase expression of the cotransporter whose function affects vascular tone. It was demonstrated that activity of the DNA methyltransferase is attenuated in hypertensive rats, while upregulated in normotensive rats [20].

The SLC12A1 (NKCC2) gene is encoded by 27 exons with alternative splicing of exon 5 which exists in three versions encoding the A, B, and F variants. Nuclear run-off assays experiments demonstrated that the kidney-specific expression of NKCC2 is due to interactions between kidney-enriched transcription factors and regulatory elements in the 5′-flanked region of the SLC12A1 gene [63]. Deletion analysis revealed the presence of positive regulatory elements controlling the NKCC2 promoter in TAL cells in an ~280-bp fragment not too far upstream from the TATA box. Those transcriptional elements include a putative Hepatocyte Nuclear Factor 1 (HNF-1) site, a GA microsatellite, two consensus CCAAT Enhancer-Binding Protein (C/EBP) binding sites, and one Enhancer Box (E-box) site. In addition, negative regulatory elements were shown to be present in a 725-bp fragment located about 1 kb upstream of the previous region. Both transcription and mRNA stability of NKCC2 are increased upon chronic metabolic alkalosis [71]. This is not unexpected as the cotransporter is a major pathway for NH_4^+ reabsorption in the medullary thick ascending limb.

Posttranslational modification

Both NKCC1 and NKCC2 are activated by an increase in the external osmolarity and a decrease in the intracellular Cl^- concentration. Activation by low Cl^- is not related to a gradient effect, but due to a Cl^--sensitive mechanism [80]. Interestingly, the two stimuli are interrelated and working in opposite directions. Indeed, an increase in external osmolarity results in cell shrinkage, which is accompanied by an increase in intracellular Cl^-. Thus, there is an activation signal due to a decrease in cell volume and an inhibition signal due to an increase in intracellular Cl^-. Whether under these conditions there is overall activation of Na–K–2Cl cotransport is a matter

of debate. Two pieces of evidence indicate that it might not be the case. First, as we discussed above, cell shrinkage induces an increase in K^+/K^+ exchange, which is neutral for net transport [26]. Second, most cells fail to exhibit a regulatory volume increase (RVI) response when exposed to a hypertonicity solution, but demonstrate RVI only when they are returned to isosmotic conditions following a hypo-osmotic challenge (for review, see [59]). Stimulation of NKCC in this case is due to the loss of Cl^- that the cells experience during volume restoration under hypotonicity. Similarly, stimulation of NKCC is sometimes observed upon mild hypotonic shock. This can also be explained by a decrease in intracellular Cl^- that occurs when low Cl^- solutions are used to decrease the external osmolarity.

There are many additional factors, e.g., physical, hormones, cytokines, and signaling cascades, that affect the activity of NKCC1 and NKCC2 [4, 14, 53, 68]. It is worth noting that not all of them affect the cotransporters directly but rather indirectly through other transport mechanisms. For instance, adenylcyclase activators (e.g., forskolin), phosphodiesterase inhibitors (IBMX), and cAMP have a profound effect on NKCC1 function in Cl^- secreting epithelia (from shark rectal gland [79] to human airway [58]). It is not at all clear, however, that the cyclic nucleotide and/or protein kinase A have a direct stimulatory effect on the cotransporter. Indeed, in this case, NKCC1 activation is likely due to stimulated Cl^- secretion on the apical membrane (i.e., through CFTR), resulting in a reduction in intracellular Cl^- and secondary activation of the cotransporter. This mode of activation likely occurs in other situations where K^+ channels and Cl^- channels activities are affected and the level of intracellular Cl^- is decreased.

Evidence that NKCC is activated by phosphorylation comes from the demonstration by John Russell that ATP depletion caused a significant decrease in Na–K–Cl transport activity in squid giant axon [1]. In addition, orthovanadate and fluoride, two inhibitors of protein phosphatases, decreased this rate of inhibition supporting the hypothesis that the cotransporter in squid axon is regulated by phosphorylation–dephosphorylation. This observation was later pursued by Bliss Forbush's group who showed that NKCC in shark rectal gland acquires phosphate at serine and threonine residues in response to forskolin and cell shrinkage stimuli [79]. The identity of the kinases remained unknown until the discovery of Ste20-kinase association with K–Cl and Na–K–2Cl cotransporters [31, 101].

The regulation of SPAK/OSR1 and of NKCC1/NKCC2 is complex and has been addressed thoroughly in a recent review [42]. Here, we will briefly summarize some of the major findings. The current working model involves WNK kinases and PKC kinase isotypes acting upstream of SPAK and OSR1 [44, 76, 113] with the best characterized activation cascade involving WNK4–SPAK. In this cascade, WNK4 and SPAK physically interact through an RFxV motif in WNK4 and the CCT/PF2 domain in SPAK. WNK4 then phosphorylates SPAK at residues T243 in the catalytic domain and S383 in the regulatory domain, resulting in the activation of the Ste20 kinase. SPAK is then able to activate and phosphorylate the Na–K–2Cl cotransporters [44, 123]. An additional protein, which seems to play a critical role in cotransporter activation, is the calcium binding protein-39 (Cab39), also called mouse protein-25 (MO25). The adaptor protein comes in two isoforms Cab39 and Cab39-like, which are the products of two related genes. Both Cab39/MO25 isoforms serve as scaffolds, stabilizing Ste20-related kinases in their close or active confirmation [8, 36]. Knockdown of Cab39/MO25 suppresses the SPAK/OSR1-mediated phosphorylation and activation of NKCC1 [36]. We recently demonstrated that Cab39 can facilitate the *trans* phosphorylation and activation of SPAK monomers, in the absence of upstream activation by WNK kinases [104]. This finding argues that the Ste20 and WNK kinases can also act independently of each other, making the interpretation of the in vivo whole animal model data much more complicated.

Important questions in the field involve the multiplicity and possible redundancy of kinases and adaptor proteins. Why do we need multiple Ste20 kinases, WNK kinases, and Cab39 proteins? One possible answer is that the homologous proteins might be expressed in different cell types, might have slightly different properties, and might differently modulate the activity of specific transport proteins. Another conceivable answer is the need for redundancy that would minimize the prospect of affecting important physiological functions. For the Ste20 kinases, we have considered the need for two Ste20 kinases and the answer is mixed. On one hand, we found SPAK and OSR1 both expressed in sensory neurons and each participating in the activation of NKCC1 [51]. On the other hand, SPAK knockout mice mainly display a distal convoluted tubule (DCT) phenotype [136], whereas OSR1 knockout mice predominantly exhibit a TAL phenotype [77]. There are also significant differences between the two kinases as OSR1 is mostly found as a full-length product, whereas SPAK in kidney medulla is also observed as smaller fragments [57, 84]. Similarly, there are some major differences between WNK kinases, both in expression patterns, as well as molecular properties [83].

Another regulator of NKCC2 function in the thick ascending limb of Henle is a protein called SORLA (Sortilin-related receptor, LDLR class A repeats-containing) and which is mostly studied in the nervous system [96]. SORLA has been shown to regulate the subcellular localization of SPAK and its ability to phosphorylate NKCC2. In SORLA knockout mice, a smaller fraction of SPAK colocalizes with NKCC2 and phosphorylation of NKCC2 is decreased, whereas the apical expression is unchanged [106].

Vasopressin is the main hormone that affects NaCl reabsorption in the TAL [88, 127]. Its infusion in live mice

increases apical expression and phosphorylation of N-terminal Thr^{96} and Thr^{101} residues of NKCC2 [54]. Vasopressin increases intracellular cAMP which phosphorylates and activates protein kinase A (PKA), this latter inducing phosphorylation (N-terminal Ser^{126} and C-terminal Ser^{874}) of rat NKCC2, leading to increase trafficking of the cotransporter to the plasma membrane [10]. While vasopressin, calcitonin, glucagon, and β-adrenergic agonists stimulate NKCC2 trafficking by a cAMP-dependent PKA pathway, atrial natriuretic peptides, endothelin, α-adrenergic agonists, and nitric oxide induce an increase in intracellular cGMP, leading to a stimulation of the phosphodiesterase 2 (PDE2), resulting in a decrease in the apical expression of NKCC2 [3]. The AMP activated kinase (AMPK) seems to also regulate NKCC2 activity by phosphorylation at Ser^{126} (as shown in a murine macula densa cell line) and at Ser^{130} in HEK cells [39, 108]. However, it is not known whether AMPK regulates NKCC2 activity in the TAL. Yeast-two-hybrid assay experiments have shown that the glycolytic enzyme, aldolase B, and the vesicle scaffolding protein, SCAMP2, both interact with the C-terminal tail of NKCC2. While an increased in aldolase B or in SCAMP2 expression decreases membrane expression of NKCC2 in co-transfected opossum kidney epithelial cells, their possible role in TAL is unknown [137]. Finally, the lipid raft-associated protein MAL/VIP17 which is expressed in the TAL interacts with the C-terminal tail to possibly decrease the endocytosis of NKCC2 [16].

Final remarks

It is clear that much progress has been made over the past 30 years in understanding the physiology of the two Na–K–2Cl cotransporters. The availability of furosemide and bumetanide as potent and rather specific inhibitors at low concentrations has greatly facilitated the identification and characterization of cotransporter function in many tissues. Likely, it is also the efficacy of furosemide and bumetanide as potent and safe inhibitors of Na^+ reabsorption in the thick ascending limb of Henle that has prevented the need to discover new inhibitory compounds. Considering the multiple roles that the NKCC1 plays outside the kidney, it would be useful to have compounds that modulate NKCC1 function without affecting NKCC2. This is particularly true when bumetanide is used in clinical settings to target NKCC1 function, with the knowledge that significant confounding effects are likely to result from blood volume reduction.

Aside from new pharmaceutical agents, crystal structures of the entire cotransporter proteins or protein domains are also in need. These structures should allow us to better understand how phosphorylation of residues in the N-terminal tail of the cotransporters results in cotransporter activation or how the structure of the tail affects the transmembrane core and the movement of the ions. The crystal structure will also give precious information on specific residues that interact with transported ions and inhibitors. These structures might also help in understanding the slippage modes of the transporter and the basis for the K^+/K^+ exchange.

As we have alluded to in this review, we have very limited information on regulation of both cotransporters at the transcriptional level. It is very unlikely that cotransporter regulation occurs mostly at the posttranslational level, as synthesis and stability of mRNA and protein must also be modulated by physiological processes. It is also clear that more and more proteins associating with the cotransporters are being identified. Whether or not all these proteins will have a significant impact on our understanding of cotransporter function is an unknown. It is clear that the discovery of Ste20 and WNK kinases has had a profound impact on our understanding of NKCC1, NKCC2, and even NCC activation, even if many of the details still need to be worked out. It is increasingly clear that these proteins are working in context-specific environments and that there are likely major differences in cotransporter regulation that are cell-type specific. The challenge will be to decipher these unique features in situations as close as physiologically possible.

Acknowledgments This work was supported by the National Institute of Diabetes and Digestive and Kidney Diseases Grant DK-093501 and the National Institute of General Medical Sciences Grant GM074771 (to E. Delpire). The authors wish to thank Dr. Kenneth Gagnon (University of Saskatchewan, Saskatoon, SK, Canada) for reading the manuscript.

References

1. Altamirano AA, Breitwieser GE, Russel JM (1988) Vanadate and fluoride effects on Na–K–Cl cotransport in squid giant axon. Am J Physiol 254:C582–C586
2. Alvarez-Leefmans FJ, Gamiño SM, Giraldez F et al (1988) Intracellular chloride regulation in amphibian dorsal root ganglion neurons studied with ion-selective microelectrodes. J Physiol Lond 406:225–246
3. Ares GR, Caceres P, Alvarez-Leefmans FJ et al (2008) cGMP decreases surface NKCC2 levels in the thick ascending limb: role of phosphodiesterase 2 (PDE2). Am J Physiol Renal Physiol 295: F877–F887
4. Ares GR, Caceres PS, Ortiz PA (2011) Molecular regulation of NKCC2 in the thick ascending limb. Am J Physiol Renal Physiol 301:F1143–F1159
5. Balakrishnan V, Becker M, Lohrke S et al (2003) Expression and function of chloride transporters during development of inhibitory neurotransmission in the auditory brainstem. J Neurosci 23:4134–4145
6. Bennett CM, Brenner BM, Berliner RW (1968) Micropuncture study of nephron function in the rhesus monkey. J Clin Invest 47: 203–216
7. Bergeron MJ, Gagnon E, Wallendorff B et al (2003) Ammonium transport and pH regulation by K(+)–Cl(−) cotransporters. Am J Physiol Renal Physiol 285:F68–F78

8. Boudeau J, Baas AF, Deak M et al (2003) MO25alpha/beta interact with STRADalpha/beta enhancing their ability to bind, activate and localize LKB1 in the cytoplasm. Embo J 22:5102–5114
9. Brumback AC, Staley KJ (2008) Thermodynamic regulation of NKCC1-mediated Cl^- cotransport underlies plasticity of GABA(A) signaling in neonatal neurons. J Neurosci 28:1301–1312
10. Caceres PS, Ares GR, Ortiz PA (2009) cAMP stimulates apical exocytosis of the renal Na(+)–K(+)–2Cl(−) cotransporter NKCC2 in the thick ascending limb: role of protein kinase A. J Biol Chem 284:24965–24971
11. Calò LA (2006) Vascular tone control in humans: insights from studies in Bartter's/Gitelman's syndromes. Kidney Int 69:963–966
12. Capasso G, Rizzo M, Evangelista C et al (2005) Altered expression of renal apical plasma membrane Na+transporters in the early phase of genetic hypertension. Am J Physiol Renal Physiol 288:F1173–F1182
13. Carmosino M, Giménez I, Caplan M et al (2008) Exon loss accounts for differential sorting of Na–K–Cl cotransporters in polarized epithelial cells. Mol Biol Cell 19:4341–4351
14. Carmosino M, Procino G, Svelto M (2012) Na+−K+−2Cl− cotransporter type 2 trafficking and activity: the role of interacting proteins. Biol Cell 104:201–212
15. Carmosino M, Rizzo F, Ferrari P et al (2011) NKCC2 is activated in Milan hypertensive rats contributing to the maintenance of salt-sensitive hypertension. Pflügers Arch Eur J Physiol 462:281–291
16. Carmosino M, Rizzo F, Procino G et al (2010) MAL/VIP17, a new player in the regulation of NKCC2 in the kidney. Mol Biol Cell 21: 3985–3997
17. Carmosino M, Rizzo F, Torretta S et al (2013) High-throughput fluorescent-based NKCC functional assay in adherent epithelial cells. BMC Cell Biol 14:16
18. Carota I, Theilig F, Oppermann M et al (2010) Localization and functional characterization of the human NKCC2 isoforms. Acta Physiol (Oxf) 199:327–338
19. Castrop H, Schnermann J (2008) Isoforms of renal Na–K–2Cl cotransporter NKCC2: expression and functional significance. Am J Physiol Renal Physiol 295:F859–F866
20. Cho HM, Lee HA, Kim HY et al (2011) Expression of Na^+–K^+–$2Cl^-$ cotransporter 1 is epigenetically regulated during postnatal development of hypertension. Am J Hypertens 24:1286–1293
21. Cui CY, Childress V, Piao Y et al (2012) Forkhead transcription factor FoxA1 regulates sweat secretion through Bestrophin 2 anion channel and Na–K–Cl cotransporter 1. Proc Natl Acad Sci U S A 109:1199–1203
22. Darman RB, Flemmer A, Forbush BI (2001) Modulation of ion transport by direct targeting of PP1 to the Na–K–Cl cotransporter. J Biol Chem 276:34359–34362
23. Darman RB, Forbush B (2002) A regulatory locus of phosphorylation in the N terminus of the Na–K–Cl cotransporter, NKCC1. J Biol Chem 277:37542–37550
24. DeFazio RA, Heger S, Ojeda SR et al (2002) Activation of A-type gamma-aminobutyric acid receptors excites gonadotropin-releasing hormone neurons. Mol Endocrinol 16:2872–2891
25. Delpire E, Days E, Mi D et al (2009) Small molecule screen identifies inhibitors of the neuronal K–Cl cotransporter KCC2. Proc Natl Acad Sci U S A 106:5383–5388
26. Delpire E, Gagnon KB (2011) Kinetics of hyperosmotically-stimulated Na–K–2Cl cotransporter in *Xenopus laevis* oocytes. Am J Physiol Cell Physiol 301:C1074–C1085
27. Delpire E, Lu J, England R et al (1999) Deafness and imbalance associated with inactivation of the secretory Na–K–2Cl co-transporter. Nat Genet 22:192–195
28. Delpire E, Rauchman MI, Beier DR et al (1994) Molecular cloning and chromosome localization of a putative basolateral Na–K–2Cl cotransporter from mouse inner medullary collecting duct (mIMCD-3) cells. J Biol Chem 269:25677–25683
29. Dietz KJ, Vogel MO, Viehhauser A (2010) AP2/EREBP transcription factors are part of gene regulatory networks and integrate metabolic, hormonal and environmental signals in stress acclimation and retrograde signalling. Protoplasma 245:3–14
30. Dixon MJ, Gazzard J, Chaudhry SS et al (1999) Mutation of the Na–K–Cl co-transporter gene Slc12a2 results in deafness in mice. Hum Mol Genet 8:1579–1584
31. Dowd BF, Forbush B (2003) PASK (proline-alanine-rich STE20-related kinase), a regulatory kinase of the Na–K–Cl cotransporter (NKCC1). J Biol Chem 278:27347–27353
32. Dzhala VI, Talos DM, Sdrulla DA et al (2005) NKCC1 transporter facilitates seizures in the developing brain. Nat Med 11:1205–1213
33. Eftekhari S, Mehvari Habibabadi J, Najafi Ziarani M et al (2013) Bumetanide reduces seizure frequency in patients with temporal lobe epilepsy. Epilepsia 54:e9–e12
34. Evans RL, Park K, Turner RJ et al (2000) Severe impairment of salivation in Na^+/K^+/$2Cl^-$ cotransporter (NKCC1)-deficient mice. J Biol Chem 275:26720–26726
35. Feldstein AE, Miller SM, El-Youssef M et al (2003) Chronic intestinal pseudoobstruction associated with altered interstitial cells of Cajal networks. J Pediatr Gastroenterol Nutr 36:492–497
36. Filippi BM, de los Heros P, Mehellou Y et al (2011) MO25 is a master regulator of SPAK/OSR1 and MST3/MST4/YSK1 protein kinases. Embo J 30:1730–1741
37. Flagella M, Clarke LL, Miller ML et al (1999) Mice lacking the basolateral Na–K–2Cl cotransporter have impaired epithelial chloride secretion and are profoundly deaf. J Biol Chem 274:26946–26955
38. Flemmer AW, Gimenez I, Dowd BF et al (2002) Activation of the Na–K–Cl cotransporter NKCC1 detected with a phospho-specific antibody. J Biol Chem 277:37551–37558
39. Fraser SA, Gimenez I, Cook N et al (2007) Regulation of the renal-specific Na^+–K^+–$2Cl^-$ co-transporter NKCC2 by AMP-activated protein kinase (AMPK). Biochem J 405:85–93
40. Gagnon KB, Delpire E (2010) Molecular determinants of hyperosmotically activated NKCC1-mediated K^+/K^+ exchange. J Physiol Lond 588:3385–3396
41. Gagnon KB, Delpire E (2010) Multiple pathways for protein phosphatase 1 (PP1) regulation of Na–K–2Cl cotransporter (NKCC1) function. The N-terminal tail of the Na–K–2Cl cotransporter serves as a regulatory scaffold for Ste20-related proline/alanine-rich kinase (SPAK) and PP1. J Biol Chem 285:14115–14121
42. Gagnon KB, Delpire E (2012) Molecular physiology of SPAK and OSR1: two Ste20-related protein kinases regulating ion transport. Physiol Rev 92:1577–1617
43. Gagnon KB, Delpire E (2013) Physiology of SLC12 transporters: lessons from inherited human genetic mutations and genetically-engineered mouse knockouts. Am J Physiol Cell Physiol 304: C693–C714
44. Gagnon KB, England R, Delpire E (2006) Volume sensitivity of cation–chloride cotransporters is modulated by the interaction of two kinases: SPAK and WNK4. Am J Physiol Cell Physiol 290: C134–C142
45. Gagnon KB, England R, Delpire E (2007) A single binding motif is required for SPAK activation of the Na–K–2Cl cotransporter. Cell Physiol Biochem 20:131–142
46. Gagnon KB, England R, Diehl L et al (2007) Apoptosis associated tyrosine kinase scaffolding of protein phosphatase 1 and SPAK reveals a novel pathway for Na–K–2C1 cotransporter regulation. Am J Physiol Cell Physiol 292:C1809–C1815
47. Gamba G, Miyanoshita A, Lombardi M et al (1994) Molecular cloning, primary structure, and characterization of two members of the mammalian electroneutral sodium–(potassium)–chloride cotransporter family expressed in kidney. J Biol Chem 269:17713–17722
48. Garg P, Martin CF, Elms SC et al (2007) Effect of the Na–K–2Cl cotransporter NKCC1 on systemic blood pressure and smooth muscle tone. Am J Physiol Heart Circ Physiol 292:H2100–H2105

49. Geck P, Heinz E (1986) The Na–K–2Cl cotransport system. J Membrane Biol 91:97–105
50. Geck P, Pietrzyk C, Burckhardt B-C et al (1980) Electrically silent cotransport of Na^+, K^+ and Cl^- in Ehrlich cells. Biochim Biophys Acta 600:432–447
51. Geng Y, Hoke A, Delpire E (2009) The Ste20 kinases SPAK and OSR1 regulate NKCC1 function in sensory neurons. J Biol Chem 284:14020–14028
52. Gerelsaikhan T, Turner RJ (2000) Transmembrane topology of the secretory Na^+–K^+–$2Cl^-$ cotransporter NKCC1 studied by in vitro translation. J Biol Chem 275:40471–40477
53. Giménez I (2006) Molecular mechanisms and regulation of furosemide-sensitive Na–K–Cl cotransporters. Curr Opin Nephrol Hypertens 15:517–523
54. Giménez I, Forbush B (2003) Short-term stimulation of the renal Na–K–Cl cotransporter (NKCC2) by vasopressin involves phosphorylation and membrane translocation of the protein. J Biol Chem 278:26946–26951
55. Gimenez I, Forbush B (2005) Regulatory phosphorylation sites in the NH_2 terminus of the renal Na–K–Cl cotransporter (NKCC2). Am J Physiol Renal Physiol 289:F1341–F1345
56. Greger R, Schlatter E (1981) Presence of luminal K^+, a prerequisite for active NaCl transport in the cortical thick ascending limb of Henle's loop of rabbit kidney. Pfluegers Arch 392:92–94
57. Grimm PR, Liu J, Coleman R et al (2011) Phosphorylation-dependent regulation of NCC is blunted in SPAK null mice ($SPAK^{-/-}$). FASEB J 25:1041.26
58. Grubb BR, Pace AJ, Lee E et al (2001) Alterations in airway ion transport in NKCC1-deficient mice. Am J Physiol Cell Physiol 281: C615–C623
59. Hoffmann EK, Lambert IH, Pedersen SF (2009) Physiology of cell volume regulation in vertebrates. Physiol Rev 89:193–277
60. Ibla JC, Khoury J, Kong T et al (2006) Transcriptional repression of Na–K–2Cl cotransporter NKCC1 by hypoxia-inducible factor-1. Am J Physiol Cell Physiol 291:C282–C289
61. Igarashi P, Vanden Heuvel GB, Payne JA et al (1995) Cloning, embryonic expression and alternative splicing of a murine kidney specific Na–K–Cl cotransporter. Am J Physiol (Renal Fluid Electrolyte Physiol) 269:F405–F418
62. Igarashi P, Vanden Heuvel GB, Quaggin SE et al (1994) Cloning, embryonic expression, and chromosomal localization of murine renal Na–K–Cl cotransporter (NKCC2). J Am Soc Nephrol 5:288
63. Igarashi P, Whyte DA, Li K et al (1996) Cloning and kidney cell-specific activity of the promoter of the murine renal Na–K–Cl cotransporter gene. J Biol Chem 271:9666–9674
64. Ikebe M, Nonoguchi H, Nakayama Y et al (2001) Upregulation of the secretory-type Na(+)/K(+)/2Cl(−)-cotransporter in the kidney by metabolic acidosis and dehydration in rats. J Am Soc Nephrol 12: 423–430
65. Isenring P, Jacoby SC, Chang J et al (1998) Mutagenic mapping of the Na–K–Cl cotransporter for domains involved in ion transport and bumetanide binding. J Gen Physiol 112:549–558
66. Isenring P, Jacoby SC, Forbush BI (1998) The role of transmembrane domain 2 in cation transport by the Na–K–Cl cotransporter. Proc Natl Acad Sci U S A 95:7179–7184
67. Jakab RL, Collaco AM, Ameen NA (2011) Physiological relevance of cell-specific distribution patterns of CFTR, NKCC1, NBCe1, and NHE3 along the crypt–villus axis in the intestine. Am J Physiol Gastrointest Liver Physiol 300:G82–G98
68. Kaplan MR, Mount DB, Delpire E et al (1996) Molecular mechanisms of NaCl cotransport. Annu Rev Physiol 58:649–668
69. Kaplan MR, Plotkin MD, Brown D et al (1996) Expression of the mouse Na–K–2Cl cotransporter, mBSC2, in the terminal IMCD, the glomerular and extraglomerular mesangium and the glomerular afferent arteriole. J Clin Invest 98:723–730
70. Kaplan MR, Plotkin MD, Lee W-S et al (1996) Apical localization of the Na–K–2Cl cotransporter, rBSC1, on rat thick ascending limbs. Kidney Int 49:40–47
71. Karim Z, Attmane-Elakeb A, Sibella V et al (2003) Acid pH increases the stability of BSC1/NKCC2 mRNA in the medullary thick ascending limb. J Am Soc Nephrol 14:2229–2214
72. Kelley LA, Sternberg MJE (2009) Protein structure prediction on the web: a case study using the Phyre server. Nat Protoc 4:363–371
73. Kim HY (2009) Renal handling of ammonium and acid base regulation. Electrolyte Blood Press 7:9–13
74. Krug AW, Papavassiliou F, Hopfer U et al (2003) Aldosterone stimulates surface expression of NHE3 in renal proximal brush borders. Pfluegers Arch 446:492–496
75. Lee MP, Ravenel JD, Hu RJ et al (2000) Targeted disruption of the Kvlqt1 gene causes deafness and gastric hyperplasia in mice. J Clin Invest 106:1447–1455
76. Li Y, Hu J, Vita R et al (2004) SPAK kinase is a substrate and target of PKCtheta in T-cell receptor-induced AP-1 activation pathway. Embo J 23:1112–1122
77. Lin SH, Yu IS, Jiang ST et al (2011) Impaired phosphorylation of Na^+–K^+–$2Cl^-$ cotransporter by oxidative stress-responsive kinase-1 deficiency manifests hypotension and Bartter-like syndrome. Proc Natl Acad Sci U S A 108:17538–17543
78. Loffing J, Schild L (2005) Functional domains of the epithelial sodium channel. J Am Soc Nephrol 16:3175–3181
79. Lytle C, Forbush BI (1992) The Na–K–Cl cotransport protein of shark rectal gland. II. Regulation by direct phosphorylation. J Biol Chem 267:25438–25443
80. Lytle C, Forbush BI (1996) Regulatory phosphorylation of the secretory Na–K–Cl cotransporter: modulation by cytoplasmic Cl. Am J Physiol Cell Physiol 270:C437–C448
81. Lytle C, McManus TJ, Haas M (1998) A model of Na–K–2Cl cotransport based on ordered ion binding and glide symmetry. Am J Physiol 274:C299–C309
82. Malnic G, Klose RM, Giebisch G (1966) Micropuncture study of distal tubular potassium and sodium transport in rat nephron. Am J Physiol 211:529–547
83. McCormick JA, Ellison DH (2011) The WNKs: atypical protein kinases with pleiotropic actions. Physiol Rev 91:177–219
84. McCormick JA, Mutig K, Nelson JH et al (2011) A SPAK isoform switch modulates renal salt transport and blood pressure. Cell Metab 14:352–364
85. McManus TJ (1987) Na, K,2Cl cotransport: kinetics and mechanism. Fed Proc 46:2377–2394
86. Monette MY, Forbush B (2012) Regulatory activation is accompanied by movement in the C terminus of the Na–K–Cl cotransporter (NKCC1). J Biol Chem 287:2210–2220
87. Moore-Hoon ML, Turner RJ (2000) The structural unit of the secretory Na^+–K^+–$2Cl^-$ cotransporter (NKCC1) is a homodimer. Biochemistry 39:3718–3724
88. Mutig K, Paliege A, Kahl T et al (2007) Vasopressin V2 receptor expression along rat, mouse, and human renal epithelia with focus on TAL. Am J Physiol Renal Physiol 293:F1166–F1177
89. Neyroud N, Tesson F, Denjoy I et al (1997) A novel mutation in the potassium channel gene KVLQT1 causes the Jervell and Lange-Nielsen cardioauditory syndrome. Nature Gen 15:186–189
90. Nezu A, Parvin MN, Turner RJ (2009) A conserved hydrophobic tetrad near the C terminus of the secretory Na^+–K^+–$2Cl^-$ cotransporter (NKCC1) is required for its correct intracellular processing. J Biol Chem 284:6869–6876
91. O'Mahony F, Toumi F, Mroz MS et al (2008) Induction of $Na^+/K^+/2Cl^-$ cotransporter expression mediates chronic potentiation of intestinal epithelial Cl−secretion by EGF. Am J Physiol Cell Physiol 294:C1362–C1370
92. O'Rourke JF, Dachs GU, Gleadle JM et al (1997) Hypoxia response elements. Oncology Res 9:327–332

93. Oppermann M, Mizel D, Kim SM et al (2007) Renal function in mice with targeted disruption of the A isoform of the Na–K–2Cl cotransporter. J Am Soc Nephrol 18:440–448
94. Pace AJ, Lee E, Athirakul K et al (2000) Failure of spermatogenesis in mouse lines deficient in the Na^+–K^+–$2Cl^-$ cotransporter. J Clin Invest 105:441–450
95. Pacheco-Alvarez D, Cristóbal PS, Meade P et al (2006) The Na^+:Cl^- cotransporter is activated and phosphorylated at the amino-terminal domain upon intracellular chloride depletion. J Biol Chem 281:28755–28763
96. Pallesen LT, Vaegter CB (2012) Sortilin and SorLA regulate neuronal sorting of trophic and dementia-linked proteins. Mol Neurobiol 45:379–387
97. Paredes A, Plata C, Rivera M et al (2006) Activity of the renal Na+−K+−2Cl−cotransporter is reduced by mutagenesis of N-glycosylation sites: role for protein surface charge in Cl−transport. Am J Physiol Renal Physiol 290:F1094–F1102
98. Payne JA, Forbush BI (1994) Alternatively spliced isoforms of the putative renal Na–K–Cl cotransporter are differentially distributed within the rabbit kidney. Proc Natl Acad Sci U S A 91:4544–4548
99. Pellikainen JM, Kosma VM (2007) Activator protein-2 in carcinogenesis with a special reference to breast cancer—a mini review. Int J Cancer 120:2061–2067
100. Peti-Peterdi J, Harris RC (2010) Macula densa sensing and signaling mechanisms of renin release. J Am Soc Nephrol 21:1093–1096
101. Piechotta K, Lu J, Delpire E (2002) Cation–chloride cotransporters interact with the stress-related kinases SPAK and OSR1. J Biol Chem 277:50812–50819
102. Plotkin MD, Kaplan MR, Peterson LN et al (1997) Expression of the Na^+–K^+–$2Cl^-$ cotransporter BSC2 in the nervous system. Am J Physiol Cell Physiol 272:C173–C183
103. Plotkin MD, Snyder EY, Hebert SC et al (1997) Expression of the Na–K–2Cl cotransporter is developmentally regulated in postnatal rat brains: a possible mechanism underlying GABA's excitatory role in immature brain. J Neurobiol 33:781–795
104. Ponce-Coria J, Gagnon KB, Delpire E (2012) Calcium-binding protein 39 facilitates molecular interaction between Ste20p proline alanine-rich kinase and oxidative stress response 1 monomers. Am J Physiol Cell Physiol 303:C1198–C1205
105. Randall J, Thorne T, Delpire E (1997) Partial cloning and characterization of *Slc12a2*: the gene encoding the secretory Na^+–K^+–$2Cl^-$ cotransporter. Am J Physiol Cell Physiol 273:C1267–C1277
106. Reiche J, Theilig F, Rafiqi FH et al (2010) SORLA/SORL1 functionally interacts with SPAK to control renal activation of Na(+)–K(+)–Cl(−) cotransporter 2. Mol Cell Biol 30:3027–3037
107. Reisert J, Lai J, Yau KW et al (2005) Mechanism of the excitatory Cl^- response in mouse olfactory receptor neurons. Neuron 45:553–561
108. Richardson C, Sakamoto K, de los Heros P et al (2011) Regulation of the NKCC2 ion cotransporter by SPAK–OSR1-dependent and -independent pathways. J Cell Sci 124:789–800
109. Russell JM (1983) Cation-coupled chloride influx in squid axon. Role of potassium and stoichiometry of the transport process. J Gen Physiol 81:909–925
110. Schlatter E, Salomonsson M, Persson AE et al (1989) Macula densa cells sense luminal NaCl concentration via furosemide sensitive Na+2Cl−K+cotransport. Pflugers Arch 414:286–290
111. Simard CF, Brunet GM, Daigle ND et al (2004) Self-interacting domains in the C terminus of a cation-Cl−cotransporter described for the first time. J Biol Chem 279:40769–40777
112. Simon DB, Karet FE, Hamdan JM et al (1996) Bartter's syndrome, hypokalaemic alkalosis with hypercalciuria, is caused by mutations in the Na–K–2Cl cotransporter *NKCC2*. Nature Gen 13:183–188
113. Smith L, Smallwood N, Altman A et al (2008) PKCdelta acts upstream of SPAK in the activation of NKCC1 by hyperosmotic stress in human airway epithelial cells. J Biol Chem 283:22147–22156
114. Somasekharan S, Tanis J, Forbush B (2012) Loop diuretic and ion-binding residues revealed by scanning mutagenesis of transmembrane helix 3 (TM3) of Na–K–Cl cotransporter (NKCC1). J Biol Chem 287:17308–17317
115. Starremans PG, Kersten FF, Knoers NV et al (2003) Mutations in the human Na–K–2Cl cotransporter (NKCC2) identified in Bartter syndrome type I consistently result in nonfunctional transporters. J Am Soc Nephrol 14:1419–1426
116. Sung K-W, Kirby M, McDonald MP et al (2000) Abnormal $GABA_A$-receptor mediated currents in dorsal root ganglion neurons isolated from Na–K–2Cl cotransporter null mice. J Neurosci 20:7531–7538
117. Takahashi N, Chernavvsky DR, Gomez RA et al (2000) Uncompensated polyuria in a mouse model of Bartter's syndrome. Proc Natl Acad Sci U S A 97:5434–5439
118. Trepiccione F, Zacchia M, Capasso G (2012) The role of the kidney in salt-sensitive hypertension. Clin Exp Nephrol 16:68–72
119. Vanderwinden JM, Liu H, De Laet MH et al (1996) Study of the interstitial cells of Cajal in infantile hypertrophic pyloric stenosis. Gastroenterology 111:279–288
120. Vanderwinden JM, Rumessen JJ, Liu H et al (1996) Interstitial cells of Cajal in human colon and in Hirschsprung's disease. Gastroenterology 111:901–910
121. Vetter DE, Mann JR, Wangemann P et al (1996) Inner ear defects induced by null mutation of the *isk* gene. Neuron 17:1251–1264
122. Vibat CR, Holland MJ, Kang JJ et al (2001) Quantitation of Na^+–K^+–$2Cl^-$ cotransport splice variants in human tissues using kinetic polymerase chain reaction. Anal Biochem 298:218–230
123. Vitari AC, Deak M, Morrice NA et al (2005) The WNK1 and WNK4 protein kinases that are mutated in Gordon's hypertension syndrome, phosphorylate and active SPAK and OSR1 protein kinases. Biochem J 391:17–24
124. Wagner CA, Devuyst O, Bourgeois S et al (2009) Regulated acid–base transport in the collecting duct. Pfluegers Arch 458:137–156
125. Wedel T, Spiegler J, Soellner S et al (2002) Enteric nerves and interstitial cells of Cajal are altered in patients with slow-transit constipation and megacolon. Gastroenterology 123:1459–1467
126. Weiner ID, Verlander JW (2011) Role of NH3 and NH4+ transporters in renal acid–base transport. Am J Physiol Renal Physiol 300:F11–F23
127. Welker P, Böhlick A, Mutig K et al (2008) Renal Na^+–K^+–Cl^- cotransporter activity and vasopressin-induced trafficking are lipid raft-dependent. Am J Physiol Renal Physiol 295:F789–F802
128. Willis WD (1999) Dorsal root potentials and dorsal root reflexes: a double-edged sword. Exp Brain Res 124:395–421
129. Wong FH, Chen JS, Reddy V et al (2012) The amino acid–polyamine–organocation superfamily. J Mol Microbiol Biotechnol 22:105–113
130. Wouters M, De Laet A, Ver Donck L et al (2006) Subtractive hybridization unravels a role for the ion co-transporter NKCC1 in the murine intestinal pacemaker. Am J Physiol Gastrointest Liver Physiol 290:G1219–G1227
131. Wu Q, Delpire E, Hebert SC et al (1998) Functional demonstration of Na–K–2Cl cotransporter activity in isolated, polarized choroid plexus cells. Am J Physiol Cell Physiol 275:C1565–C1572
132. Xu J-C, Lytle C, Zhu TT et al (1994) Molecular cloning and functional expression of the bumetanide-sensitive Na–K–2Cl cotransporter. Proc Natl Acad Sci U S A 91:2201–2205
133. Yamamoto Y, Matsubara A, Ishii K et al (2002) Localization of gamma-aminobutyric acid A receptor subunits in the rat spiral ganglion and organ of Corti. Acta Otolaryngol 122:709–714
134. Yamashita A, Singh SK, Kawate T et al (2005) Crystal structure of a bacterial homologue of Na+/Cl−−dependent neurotransmitter transporters. Nature 437:215–223
135. Yang T, Huang YG, Singh I et al (1996) Localization of bumetanide- and thiazide-sensitive Na–K–Cl cotransporters

along the rat nephron. Am J Physiol (Renal Physiol) 271:F931–F939
136. Yang SS, Lo YF, Wu CC et al (2010) SPAK-knockout mice manifest Gitelman syndrome and impaired vasoconstriction. J Am Soc Nephrol 21:1868–1877
137. Zaarour N, Defontaine N, Demaretz S et al (2011) Secretory carrier membrane protein 2 regulates exocytic insertion of NKCC2 into the cell membrane. J Biol Chem 286:9489–9502
138. Zdebik AA, Wangemann P, Jentsch TJ (2009) Potassium ion movement in the inner ear: insights from genetic disease and mouse models. Physiology (Bethesda) 24:307–316
139. Zhang LL, Delpire E, Vardi N (2007) NKCC1 does not accumulate chloride in developing retinal neurons. J Neurophysiol 98:266–277
140. Zhu L, Polley N, Mathews GC et al (2008) NKCC1 and KCC2 prevent hyperexcitability in the mouse hippocampus. Epilepsy Res 79:201–212